Ablation of the tail of the ventral tegmental area compensates symptoms in an experimental model of Parkinson's disease

Fanny Faivre[a,1], María-José Sánchez-Catalán[a,b,1], Sandra Dovero[c,d], Simone Bido[c,d], Anil Joshi[a,e], Erwan Bezard[c,d], Michel Barrot[a,*]

[a] Centre National de la Recherche Scientifique, Université de Strasbourg, Institut des Neurosciences Cellulaires et Intégratives, F-67000 Strasbourg, France
[b] Unitat Predepartemental de Medicina, Universitat Jaume I Castelló de la Plana, Spain
[c] Université de Bordeaux, Institut des Maladies Neurodégénératives, UMR 5293, F-33000 Bordeaux, France
[d] Centre National de la Recherche Scientifique, Institut des Maladies Neurodégénératives, UMR 5293, F-33000 Bordeaux, France
[e] Department of Endocrinology and Metabolism, Amsterdam University Medical Centers, University of Amsterdam, Amsterdam, Netherlands

ARTICLE INFO

ABSTRACT

Parkinson's disease is a neurodegenerative disorder partly caused by the loss of the dopamine neurons of the nigrostriatal pathway. It is accompanied by motor as well as non-motor symptoms, including pain and depression. The tail of the ventral tegmental area (tVTA) or rostromedial tegmental nucleus (RMTg) is a GABAergic mesopontine structure that acts as a major inhibitory brake for the substantia nigra *pars compacta* (SNc) dopamine cells, thus controlling their neuronal activity and related motor functions. The present study tested the influence of suppressing this tVTA brake on motor and non-motor symptoms in a rat model of Parkinson's disease. Using behavioral approaches, we showed that male Sprague-Dawley rats with bilateral and partial 6-hydroxydopamine SNc lesion displayed motor impairments in the rotarod test, impairments that were no more present following a co-lesion of the tVTA. Using a larger set of behavioral tests, we then showed that such SNc lesion also led to non-motor symptoms, including lower body weight, lower mechanical nociceptive thresholds in the forceps test and lower thermal nociceptive thresholds in the incremented hot-plate test, and a decreased sucrose preference in a 2-bottle choice paradigm. The excitotoxic co-lesion of the tVTA led to compensation of body weight, mechanical nociceptive thresholds and anhedonia-like behavior. These findings illustrate the major influence that the tVTA exerts on the dopamine system, modulating the motor and non-motor symptoms related to a partial loss of dopamine cells.

1. Introduction

Parkinson's disease is a common and progressive neurodegenerative disorder, mainly characterized by the loss of dopaminergic neurons of the substantia nigra *pars compacta* (SNc) in the midbrain and by the presence of cytoplasmic protein aggregates of α-synuclein (Lewy bodies) in the affected brain areas. The neurodegeneration in Parkinson's disease leads to a triad of motor symptoms including bradykinesia, muscle rigidity and resting tremor. Likewise, a variety of non-motor symptoms are related to the progression of the disease, including sleep disorders, gastrointestinal and autonomic symptoms (nausea, constipation), sensory symptoms (olfactory impairment), pain

and neuropsychiatric symptoms (depression, anxiety) (Blanchet and Brefel-Courbon, 2017; Chaudhuri et al., 2006; Faivre et al., 2019; Park and Stacy, 2009). The clinical diagnosis is mainly based on the motor symptoms which are noticeable when the disease is already advanced, whereas pain and emotional disturbances can be among prodromal symptoms whose early identification might facilitate early diagnosis and treatment (Antonini et al., 2018; Marsili et al., 2018).

Various animal models of Parkinson's disease have been established, attempting to reproduce parkinsonian-like symptoms (for review, see Faivre et al., 2019), including motor and non-motor ones (Vingill et al., 2018). The 6-hydroxydopamine (6-OHDA) models have been classically used in Parkinson's disease studies, as the direct brain administration of

---

this toxin allows a destruction of dopamine neurons terminals and soma (Ungerstedt, 1968), hence leading to motor symptoms comparable to those appearing in humans (Gubellini and Kachidian, 2015; Ungerstedt, 1968), as well as to non-motor symptoms (Bonito-Oliva et al., 2014; Faivre et al., 2019). Moreover, partial lesions with 6-OHDA might also provide a model of early stages of the disease (Gubellini and Kachidian, 2015).

The tail of the ventral tegmental area (tVTA) (Kaufling et al., 2009; Perrotti et al., 2005), also named rostromedial tegmental nucleus (RMTg) (Jhou et al., 2009a, 2009b), is a GABAergic mesopontine structure that exerts an important inhibitory control on the midbrain dopamine neurons of the ventral tegmental area (VTA) and the SNc (Bourdy and Barrot, 2012; Sanchez-Catalan et al., 2014). The tVTA functions have been explored in the response to drugs of abuse (Kaufling et al., 2010a, 2010b; Jalabert et al., 2011; Lecca et al., 2011, 2012; Matsui and Williams, 2011; Jhou et al., 2012, 2013; Kaufling and Aston-Jones, 2015), in avoidance behaviors (Jhou et al., 2009a; Li et al., 2019; Sánchez-Catalán et al., 2017; Stamatakis and Stuber, 2012), in reward prediction error (Hong et al., 2011) and in the control of motor function (Bourdy et al., 2014). Regarding the tVTA role in motor function, a tVTA-nigrostriatal pathway has been described, as well as the inhibitory electrophysiological influence of the tVTA on SNc dopamine neurons (Bourdy et al., 2014). At behavioral level, the tVTA ablation can compensate the amphetamine-induced rotation bias after partial ipsilateral lesion of the SNc (Bourdy et al., 2014). Moreover, animals with a bilateral ablation of the tVTA display increased motor performances and better motor skill learning compared to sham animals in a rotarod task (Bourdy et al., 2014). Thus, the experimental evidence supports an influence of the tVTA on basal ganglia circuitry.

In the present study, we explored whether a bilateral tVTA ablation could improve the deficit in motor coordination observed following the bilateral partial loss of SNc dopamine neurons. We then completed the behavioral analysis of the model to include some non-motor symptoms, and we tested the impact of tVTA lesion on some of these symptoms.

2. Material and methods

2.1. Ethical approval

All procedures involving animals were performed in accordance with the Centre National de la Recherche Scientifique (CNRS) and the European Union directive (2010/63/EU) on the protection of animals used for scientific purposes. Experiments were approved by the Institutional Animal Care and Use Committee of Strasbourg (CREMEAS – France; #02051.01).

2.2. Animals

Experiments were performed in adult male Sprague-Dawley rats (Janvier, France). The rats were habituated to the facilities for at least one week before starting the procedures, and were 7–9 weeks old (*i.e* 200-300 g) at surgery time. They were housed 2 per cage, under standard conditions (22 °C, 12-h light/dark cycle) and were provided with food and water *ad libitum*.

2.3. Drugs

Ibotenic acid (1% in phosphate-buffered saline (PBS) 0.1 M; 0.3 μL per side) was injected bilaterally into the tVTA using Hamilton syringes with 33-gauge needles. The syringe plunger was manually pushed at a rate of 0.05 μL every 30 s. The 6-hydroxydopamine hydrochloride (6-OHDA; 2.5 μg/μL in 0.9% NaCl with 0.01% ascorbic acid) was injected bilaterally into the SNc (1.75 μL per side for partial lesion). The syringe plunger was manually pushed at a rate of 0.5 μL every 30 s and 0.25 μL for the last push. Needles were then let in place 5 min before removal to allow solution diffusion. When no lesion was performed (Sham groups), the needle was just placed in the target brain area but nothing was injected.

2.4. Surgical procedures

2.4.1. Experiment 1

Rats were randomly assigned to 4 groups for bilateral surgery: control (no lesion either of the tVTA or the SNc), SNc lesion (6-OHDA into the SNc and no lesion in the tVTA), tVTA lesion (ibotenic acid into the tVTA and no lesion in the SNc), and double lesion (both tVTA and SNc lesion). Animals were anaesthetized under sodium pentobarbital (50 mg/kg, intraperitoneal (i.p.); Ceva Santé Animale, Libourne, France). The depth of anesthesia was controlled during surgery by checking pedal reflex and a third of the initial dose was reinjected if necessary. Before placing the animal in a stereotaxic frame (David Kopf, Tujunga, CA), a local anesthetic (bupivacaine, 25 mg/kg; Mylan, Saint Priest, France) and an anti-inflammatory drug (Metacam®, 1 mL/kg; Boehringer Ingelheim/Rhein, Germany) were injected subcutaneously. A hydrating gel (Ocry-gel, TVM Laboratories, Lempdes, France) was regularly applied on animal's eyes to avoid dehydration. Stereotaxic coordinates relative to bregma were adjusted to the animal weight, coordinates (in mm) were as follows (Paxinos and Watson, 2014): tVTA, anteroposterior (AP) = − 6.6, lateral (L) = ± 1.3, ventral (V) = − 7.6, ± 6° lateral angle and SNc, AP = − 5.2, L = ± 2.2, V = −7.7. Verticality was taken from the dura. After injection, the needle was left in place for 5 min before removal. Following surgery, animals were kept under a warming lamp for anesthesia recovery and later returned back to the home cage. An oral anti-inflammatory treatment (Metacam®, 1 mL for 100 mL of water solution; Boehringer, Ingelheim/Rhein, Germany) and a special palatable food (gel-diet mixed with baby food) were available for 3 days post-surgery. After post-mortem control for the extent of nigrostriatal lesion, 36 rats (spread over 3 experimental waves) were retained for inclusion into behavioral analysis of tVTA impact on motor coordination.

2.4.2. Experiment 2

Rats were randomly distributed in 2 groups: control (no lesion) and SNc lesion (6-OHDA into the SNc). The surgical procedure was as described above for *experiment 1*. After post-mortem control for the extent of the 6-OHDA-induced lesion, 21 rats were retained for inclusion into behavioral analysis.

2.4.3. Experiment 3

Rats were randomly assigned to 4 groups: control (no lesion), SNc lesion (6-OHDA), tVTA lesion (ibotenic acid), and double lesion. The surgical procedure was as described above for *experiment 1*. After post-mortem control for the extent of lesion, 25 rats (spread over 2 experimental waves) were retained for inclusion into behavioral analysis assessing the impact of tVTA lesion on non-motor symptoms.

2.5. Behavioral tests

2.5.1. Rotarod

To evaluate the effect of lesions on motor coordination (*experiment 1*), animals were tested on the rotarod (Roto-Rod Series 8, IITC Life Science). Before surgery, they underwent training sessions, with one habituation session to the rotarod (5 min, 5 RPM) and three consecutive sessions over three consecutive days under an accelerating speed ramp (0–45 RPM, 180 s). After 7 to 10 days post-surgery, rotarod performance was evaluated with three sessions over three consecutive days under accelerated speed as described above. For each of the test days, results are expressed as the mean latency to fall for trials on this day.

To control for motor deficits in 6-OHDA animals (*experiment 2*), rotarod (Roto-Rod Series 8, IITC Life Science) performance was evaluated on week 12 after surgery, testing animals with four fixed speed (5, 10, 15 and 20 RPM) and measuring the latency to fall.

2.5.2. Forceps

The mechanical sensitivity (*experiments 2 & 3*) was evaluated using

digital calibrated forceps also referred to as rodent pincher-analgesia meter (Société Bioseb, Chaville, France) as previously described (Luis-Delgado et al., 2006). Shortly, animals were loosely maintained on the bench surface, using a towel in order to mask the eyes and limit influences from environmental stimulations. The tips of the forceps were placed in the middle of the hind paw and the experimenter applied incremented force by hand until paw withdrawal. Measures were repeated 3 times for each hind paw during each testing session, and results were expressed as the mean (in g) of the 3 measures. For *experiment 3*, a baseline was done before surgery. Weekly values after surgery correspond to the average of the values for both paws.

2.5.3. Tail Flick

The tail flick reflex (*experiment 2*) was evaluated with a tail flick analgesia meter (52–495, Harvard apparatus, Massachusetts, United States). Animals were loosely maintained on the apparatus, using a towel in order to mask the eyes and limit influences from environmental stimulations. Light from the halogen lamp of the apparatus was focused on the tail of the animal, and the tail flick reflex was automatically detected and expressed as latency (seconds). The cut off time was set at 10 s to avoid tissue damage.

2.5.4. Hot plate

The response latency to a nociceptive heat stimulus (*experiment 2*) was evaluated using a hot plate (Series 8, IITC Life Science, Woodland Hill, California). The apparatus temperature was set at 52 °C ± 0.1 °C. The latency to the first hind paw licking or withdrawal was considered as nociceptive response. The cut off time was set at 15 s to avoid paw damage.

2.5.5. Dynamic hot plate

Thermal sensitivity in the dynamic hot plate (DHP) (*experiment 2*) was assessed as previously described (Yalcin et al., 2009). Animals were placed on a hot plate (BIO-CHP, Société Bioseb, Chaville, France) set at 30° ± 0.1 °C, and the plate temperature increased up to 40 °C with 1 °C.min^{-1} computer-controlled speed. During each degree interval, the number of hind paw lickings, paw withdrawals and rearing was scored. Results are expressed as number of responses for each degree interval, and as cumulative responses between 33 and 36 °C at 5 and 14 weeks post-surgery time-points.

2.5.6. Sucrose consumption test

Before surgery, animals were habituated for 48 h to have two water bottles on their home cages, followed by 48 h to sugar taste with two bottles of 1% sucrose (Euromedex, France). On the test day, animals were individually housed and underwent water deprivation at 12 AM and were then allowed to choose between sugar and water during the testing time period (from 6 to 7 PM). Bottles were randomly positioned and were weighted before and after the test to evaluate sucrose consumption and preference. Solution consumption over 50% of total intake was considered as preference for the corresponding bottle. At the end of the experiments, the amount of water consumption (2 bottles of water) was also evaluated during 1 h as control (*experiments 2 & 3*). For *experiment 3*, a baseline was done before surgery.

2.6. Tissue preparation

2.6.1. Experiments 1 and 3

At the end of the experiments, rats were anaesthetized with sodium pentobarbital overdose (Dolethal®, 800 mg/kg, Vetoquinol S.A., Lure, France). The depth of anesthesia was controlled for by checking pedal reflex and animals were reinjected if necessary. Heads were isolated, and brains were collected and placed in a paraformaldehyde/glycerol solution (4% PFA, 20% glycerol in phosphate buffer) overnight at 4 °C and then kept at 4 °C in phosphate buffer saline solution (PBS, 0.1 M, pH 7.4). After further cryopreservation (20% glycerol in PBS 0.1 M,

pH 7.4), coronal brain sections (40 μm) were obtained using a microtome with frozen station (SM 2000 R, Leica) and were serially collected in PBS (0.1 M, pH 7.4).

2.6.2. Experiment 2

At the end of the experiment, rats were rapidly anaesthetized with sodium pentobarbital overdose (Dolethal®, 800 mg/kg, Vetoquinol S.A., Lure, France). The depth of anesthesia was controlled for by checking pedal reflex and animals were reinjected if necessary. Using a peristaltic pump, rats were transcardially perfused with 100 mL of phosphate buffer (0.1 M, pH 7.4) followed by 500 mL of PFA/glutaraldehyde solution (2% PFA, 0.2% glutaraldehyde in 0.2 M phosphate buffer). Brains were collected, postfixed overnight with 2% PFA and then cryoprotected in PBS containing 20% sucrose, frozen by immersion in a − 45 °C isopentane bath before being stored at −80 °C until cutting. 50 μm thickness sections of both striatal and SNc levels were made by a Leica CM3050S cryostat (LEICA microsystems, Wetzler, Germany) at −20 °C.

2.7. Immunohistochemistry

2.7.1. Experiments 1 and 3

Immunohistochemistry was performed as previously described (Bourdy et al., 2014). Sections were washed in PBS (3 × 10 minutes), incubated for 20 min in a 1% H_2O_2/50% ethanol solution for peroxidase extinction, washed in PBS (3 × 10 minutes), and incubated with a solution of PBS-Triton X100 (0.3%) with donkey serum (5%) during 45 min. Then, sections were incubated overnight with a solution of PBS-Triton X100 (0.3%) with donkey serum (1%) and the primary antibody (NeuN, #MAB377, Millipore, 1/2500; or tyrosine hydroxylase (TH), #MAB318, Millipore-Chemicon, 1/2000). All steps were performed on rotary shaker at room temperature. After 3 × 10 minutes washing in PBS, sections were incubated with a biotinylated donkey anti-mouse secondary antibody (1/400, #BA2001, Vector Laboratories) and 1% donkey serum for 90 min. After PBS rinsing (3 × 10 minutes), the biotin system was amplified with the avidin-biotin-peroxidase complex (ABC; ABC Elite, 0.2% A and 0.2% B; Vector Laboratories) in PBS during 90 min. Sections were rinsed with 0.05 M Tris-HCl buffer (TB; pH 7.5; 3 × 10 min) and the bound peroxidase was revealed by incubation in 0.025% 3.3′-diaminobenzidine tetrahydrochloride (DAB, Sigma), 0.0006% H_2O_2 (Sigma) in TB for approximately 5 to 10 minutes. The reaction was stopped by 2 × 10 minutes of TB and 2 × 10 minutes of PBS washing. Sections were then serially mounted on Superfrost® slides (VWR), air-dried, dehydrated in graded alcohols baths (1 × 70%, 1 × 95% and 2 × 100%), cleared in Roti-Histol (Carl Roth, Karlsruhe, Germany) and coverslipped with Eukitt. Evaluation of the lesion was performed using a Nikon Eclipse 80i microscope and pictures were taken with a digital camera (CX 9000, MBF biosciences).

2.7.2. Experiment 2

Midbrain and striatal serial sections were processed for TH immunohistochemistry (Bourdenx et al., 2015). Serial free-floating sections were incubated with rabbit monoclonal TH antibody (Abcam, #ab75875, 1/5000) for one night at room temperature and revealed by an anti-mouse peroxidase EnVision™ system followed by DAB staining. SNc and VTA sections were mounted on gelatinized slides, counterstained with a 0.1% cresyl violet solution, dehydrated and coversliped; while striatal sections were mounted on gelatinized slides and coversliped only.

2.8. Evaluation of the lesions

The extent of the tVTA and SNc lesions was evaluated by visualization of NeuN and TH immunohistochemistries repectively.

For animals of *experiment 2*, TH level in the striatum was semi-quantified by comparing TH immunostaining density in sections of

lesioned animals *versus* the mean density in control animals. Sections were scanned in an Epson expression 10000XL high-resolution scanner. Images were then analyzed in Image J software (Bethesda, MD, USA) to measure mean grey level in the delineated striatum, as previously described (Bourdenx et al., 2015).

TH-positive SNc or VTA cells were counted by stereology, blind with regard to the experimental condition, using a Leica DM6000B motorized microscope coupled with the Mercator Pro software (ExploraNova, La Rochelle, France), as previously described (Bourdenx et al., 2015). The SNc or VTA were delineated for each section and probes for stereological counting were applied to the map obtained (sampling 1–6, dissector window 80 × 60 μm, spacing 240 × 180 μm). Each TH-positive cell with its nucleus included in the probe or intersecting any of the acceptance lines was counted. The optical fractionator method was finally used to estimate the total number of TH-positive cells in the SNc of each animal.

2.9. Data analysis

Results are expressed as mean ± standard error of the mean (SEM). Statistical tests were performed using STATISTICA 13 software (Statsoft, Tulsa, OK, USA). We used a student *t*-test for a two group comparison; and multifactor analysis of variance (ANOVA) with, depending on the experiment, time, speed (RPM) or temperature considered as within factors (*i.e.* repeated measures) and surgery groups as between factors (*i.e.* independent groups), followed by Duncan *post-hoc* when applicable. The significance level was set at $P < .05$.

3. Results

3.1. Bilateral tVTA ablation compensated motor impairment related to partial loss of SNc dopamine cells (experiment 1)

We previously reported (Bourdy et al., 2014) that the tVTA can modulate motor performance in a rotarod task, and that a tVTA lesion prevented the amphetamine-induced ipsilateral rotation bias observed after partial unilateral SNc lesion. Based on these findings, we tested here the impact of a bilateral lesion of the tVTA on motor impairments observed in a model of Parkinson's disease. To this end, we injected bilaterally 6-OHDA into the SNc and/or ibotenic acid into the tVTA. This resulted in a partial loss of dopaminergic cells in the SNc and a large neuronal death into the tVTA, as illustrated by TH and NeuN immunostaining respectively (Fig. 1A). Animals were trained in the rotarod task before surgery. All of them completed the training phase, and the effect of the lesions on motor performance was tested for three consecutive days, 7 to 10 days after surgery. Bilateral SNc lesion induced a motor deficit in the rotarod task on test days 2 and 3 compared to sham animals ($F_{6,60} = 23.40$, $P = .000119$; *post hoc* day 2: $P = .027$, day 3: $P = .0086$). Conversely, a bilateral tVTA lesion induced an increase in motor performance over test days compared to control animals (day 2: $P = .0041$, day 3: $P = .000038$). The concomitant lesions of the SNc and the tVTA resulted in an apparently additive effect, thus suppressing the motor impairment by leading to performances that are similar to the ones observed in the control group (SNc/tVTA lesion *vs* sham: day 1: $P = .9$, day 2: $P = .83$, day 3: $P = .19$; SNc/tVTA lesion *vs* SNc lesion: day 1: $P = .08$, day 2: P = .02, day 3: $P = .001$; SNc/tVTA lesion *vs* tVTA lesion: day 1: $P = .09$, day2: P = .004, day 3: $P = .000096$) (Fig. 1B, C).

3.2. Partial bilateral SNc ablation induced motor and non-motor parkinsonian-like symptoms (experiment 2)

In Parkinson's disease, patients suffer not only from motor deficits but also from non-motor symptoms, such as pain and depression (Faivre et al., 2019). Before testing whether tVTA lesion may also affect these symptoms in the lesion model of Parkinson's disease, we first

characterized the occurrence of these non-motor symptoms. The evaluation of the lesion conducted at the end of the experiment showed that 6-OHDA animals displayed a partial SNc bilateral lesion (left SNc −79.6 ± 7.5% and right SNc −84.3 ± 5% of lesion compared to sham animals) ($F_{1,19} = 130.38$, $P = 6*10^{-10}$; *post hoc* left: $P = .000062$; right: P = .000062), associated with a partial bilateral loss of TH-positive fibers in the striatum, as evaluated by a decrease in grey level density (left striatum −62 ± 8.6% and right striatum −68.3 ± 4.9%) ($F_{1,19} = 66.77$, $P = 1.2*10^{-7}$; *post hoc* left: $P = .000066$; right: P = .000066) as previously described (Gómez-Paz et al., 2018). We also observed some loss of VTA dopamine cells (left VTA −21.3 ± 5.9% and right VTA -17.4 ± 6.5%; overall $F_{1,19} = 5.2$, $P = .03$) and a mild decrease in the TH immunostaining in the nucleus accumbens (NAc) (left NAc −11.6 ± 2.8% and right NAc −10.8 ± 4.5%; overall $F_{1,19} = 4.5$, $P = .047$), although non-significant when considering each side (VTA: *post hoc* left: $P = .078$; right: $P = .12$; NAc TH: *post hoc* left: P = .07; right: $P = .068$) (Fig. 2A).

Near the end of the experiment (12 weeks), we tested motor performance using the rotarod test (Fig. 2B). Two animals (one control and one lesion) jumped deliberately and were excluded from the results of this test. Lesioned animals performed similarly to controls at an unchallenging rotarod speed (5 RPM: $P = .61$). When rotarod speed was increased, we observed a deficit in the lesioned rats ($F_{1.17} = 4.73$, $P = .044$) compared to the unchallenging condition (5 RPM). While lesioned animals still performed similarly to controls at 10 RPM (*post hoc*: $P = .92$), they were significantly less performant at 15 RPM (*post hoc*: P = .047) and at 20 RPM (*post hoc*: $P = .008$) (Fig. 2B).

As previously described (Sakai and Gash, 1994), the bilateral 6-OHDA lesion induced a deficit in body weight increase (Fig. 2C) ($F_{1,19} = 11.72$, $P = .0028$; *post hoc* week (W) 0: $P = .46$, W1: $P = .013$, W2: $P = .0019$, W3: $P = .0035$, W4: $P = .0045$, W5: P = .004, W12: $P = .00021$).

To test pain sensitivity, we first evaluated mechanical thresholds of paw withdrawal using the forceps test (Luis-Delgado et al., 2006). The SNc lesion group had lower mechanical paw withdrawal thresholds all over the sessions compared to the control group ($F_{1,19} = 39.53$, $P = 5*10^{-6}$; *post hoc* W2: $P = .0013$, W3: $P = .0024$, W4: $P = .00028$, W5: P = .001, W12: $P = .000054$) (Fig. 2D). As the animal weight or age may influence results in this test (Luis-Delgado et al., 2006), we tested whether a relation was present between animals' weight and paw withdrawal thresholds at each time-point. No significant correlation was observed between the weight of animals and their mechanical threshold for paw withdrawal (R^2 comprised between 0.085 and 0.385). In order to evaluate the thermal sensitivity to heat of the animals, we performed three different tests: the tail flick test, the hot plate test and the dynamic hot plate test. The tail flick is a spinal reflex that can be influenced by supraspinal descending controls (Barrot, 2012). In this test, SNc lesioned animals showed a delayed tail-flick latency at only week 13 after surgery ($F_{1,19} = 12.85$, $P = .0015$; *post hoc* W13: $P = .00013$, W2 to W12: P between 0.06 and 0.52) (Fig. 2E). In the hot plate test (Fig. 2F) which provides a more integrated supraspinal response, we observed a global group difference ($F_{1,19} = 5.27$, $P = .03$) when including all time points together, suggesting heat hypersensitivity in animals with SNc lesion. However, *post hoc* analysis was significant at none of the individual time points (W2: $P = .13$, W3: $P = .15$, W4: $P = .06$, W5: $P = .2$, W12: $P = .21$, W13: $P = .11$), which, together with tail flick data, suggested a potential conflict between alterations in reflex and nociceptive responses. Thus, we considered using the dynamic hot plate test to have a more precise estimate of heat sensitivity. Indeed, the slow increase in temperature allowed minimizing the influence of reflex speed on the overall behavioral responses. In the dynamic hot plate test, SNc lesioned animals displayed a thermal allodynia, *i.e.* nociceptive responses at normally non-nociceptive temperatures ($F_{1,19} = 14.29$, P = .0013; *post hoc*: $P = .05$ at 35 °C and $P = .016$ at 36 °C at week 14) (Fig. 2G). This thermal allodynia was further highlighted by considering the cumulative behavioral responses
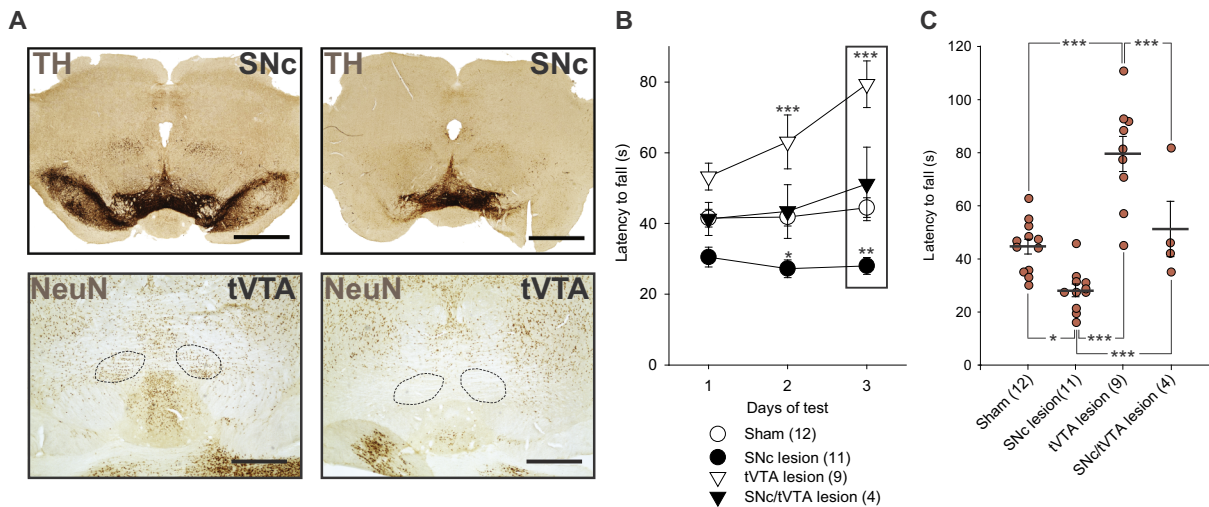
Fig. 1. Motor performance in the rotarod task after bilateral SNc and/or tVTA lesion. Animal underwent SNc lesion (6-OHDA) and/or tVTA excitotoxic lesion (ibotenic acid). 7 to 10 days after the lesion, motor performance was tested in the rotarod test. (A) Histological evidence for bilateral SNc and tVTA lesion with TH and NeuN immunostaining respectively. Scale bars, TH pictures = 1 mm; NeuN pictures = 400 μm. (B) Latency to fall is altered in animals with SNc or tVTA lesion but not in animals with concomitant bilateral SNc/tVTA lesion. (C) Individual distribution of latency to fall on the third test day. Values are presented as mean ± SEM. (*, $P < .05$; **, $P < .01$; ***, $P < .005$). The number of animals is given between brackets. Scatter plots indicate individual data points. Abbreviation: NeuN, neuronal nuclei; SNc, substantia nigra pars compacta; TH, tyrosine hydroxylase; tVTA, tail of the ventral tegmental area.

between 33 and 36 °C ($F_{1,19} = 21.83$, $P = .00017$; *post hoc* W5: $P = .013$, W14: $P = .00037$) (Fig. 2G).

Finally, we performed a sucrose preference test to assess anhedonia-like behavior as symptom of depressive-like behavior. SNc lesioned animals showed a decreased sucrose preference 4 weeks after surgery, and a lack of preference between sucrose and water at 13 weeks post-surgery ($F_{1,19} = 14.59$, $P = .0011$; *post hoc* W4: P = .01, W13: $P = .0022$). Moreover, when the total sucrose consumption was considered, it showed that SNc lesioned animals had a decreased sucrose consumption ($F_{1,19} = 8.41$, $P = .009$) at 3 (*post hoc*: $P = .034$), 5 ($P = .004$) and 13 weeks after surgery ($P = .0076$), whereas no difference in water consumption was observed (Fig. 2H).

3.3. SNc/tVTA co-ablation improved parkinsonian-like symptoms (experiment 3)

Based on these results, we chose the most robust test for assessing nociceptive-related responses (*i.e.* mechanical thresholds), and the sucrose preference test for assessing anhedonia-like behavior, in order to evaluate the impact of a bilateral tVTA lesion on non-motor symptoms in the model of Parkinson's disease. As observed in the *experiment 2,* animals with a bilateral SNc lesion had a lower body weight than sham animals ($F_{3,21} = 6.51$, $P = .0028$; *post hoc* W1: $P = .047$, W2: $P = .034$, W3: $P = .0067$, W4: $P = .0097$, W5: $P = .0076$, W6: $P = .0044$, W7: $P = .0028$), but also than tVTA lesioned animals at 3, 5, 6 and 7 weeks post-surgery (W1: $P = .31$, W2: $P = .065$, W3: $P = .017$, W4: $P = .056$, W5: $P = .019$, W6: $P = .029$, W7: $P = .009$) and than animals with double lesion since week 4 (W1: $P = .44$, W2: $P = .07$, W3: $P = .058$, W4: P = .004, W5: P = .004, W6: $P = .0005$, W7: $P = .00016$) (Fig. 3B), which showed that the double lesion allowed to compensate for body weight deficits related to SNc cell loss.

Likewise, SNc lesioned animals had a lower mechanical threshold in the forceps test compared to sham animals, tVTA lesioned animals and SNc/tVTA lesioned animals ($F_{3,21} = 14.99$, $P = .000019$; *post hoc* SNc lesion *vs* sham, W2: $P = .013$, W3: P = .007, W4: P = .007, W5: $P = .00012$; *post hoc* SNc lesion *vs* tVTA lesion, W2: $P = .11$, W3: P = .005, W4: P = .009, W5: $P = .00027$; *post hoc* SNc lesion *vs* SNc/tVTA lesion, W2: P = .004, W3: $P = .00043$, W4: $P = .0033$, W5: $P = .0062$) (Fig. 3C). While tVTA lesion did not influence *per se* the nociceptive response, it allowed suppressing the impact of SNc cell loss.

As observed in the *experiment 2*, no significant correlation was present between the body weight of the animals and their mechanical threshold (R^2 comprised between 0.00002 and 0.27) (data not shown).

Regarding the sucrose preference test, SNc lesioned animals showed a decreased preference for sucrose solution which became significant at the end of the experiment ($F_{3,21} = 3.50$, P = .03; *post hoc* W5: $P = .032$). No difference was observed in the volume of water consumed ($F_{3,21} = 0.64$, $P = .60$). Otherwise, the tVTA lesion and the co-lesioned animals showed no difference when compared to control animals, showing that double lesion compensated for SNc lesion impact (Fig. 3D).

4. Discussion

In the present study, we showed that a partial bilateral lesion of the SNc leads to both motor and non-motor symptoms, such as lower body weight, mechanical and thermal hypersensitivity, a potential slowdown of the tail reflex motor response and a depressive-like symptom in a sucrose preference test. By exploring the impact of the tVTA on those parkinsonian-like symptoms, we further showed that the co-lesion of the tVTA improved both motor and non-motor symptoms.

6-OHDA models have been widely used to study Parkinson's disease. This neurotoxin causes the loss of catecholaminergic containing cell bodies and terminals (Ungerstedt, 1968) by the production of reactive oxygen species. Noradrenergic and serotoninergic neuroprotection may be used to obtain exclusive dopamine cell damage; however, it has been suggested that models without such neuroprotection might provide better modelling of Parkinson's disease (Bezard et al., 2013). 6-OHDA has mostly been injected unilaterally, into the SNc or the medial forebrain bundle, to elicit the loss of dopamine neurons in animals. Conversely, partial bilateral lesion better mimic the neuropathy of Parkinson's disease in human in which there is usually an incomplete bilateral destruction of dopamine neurons in the SNc (German et al., 1989) and a more limited loss of some sensitive neurons in the VTA (Alberico et al., 2015). However, such bilateral lesion may cause aphagia and adipsia, leading to decreased body weight and even the death of the animals (Bezard and Przedborski, 2011; Bové et al., 2005; Dauer and Przedborski, 2003). The partial bilateral SNc lesion combined with careful postsurgical care, including rehydration with saline solution and special palatable food inside the cage, helped preventing animal loss.
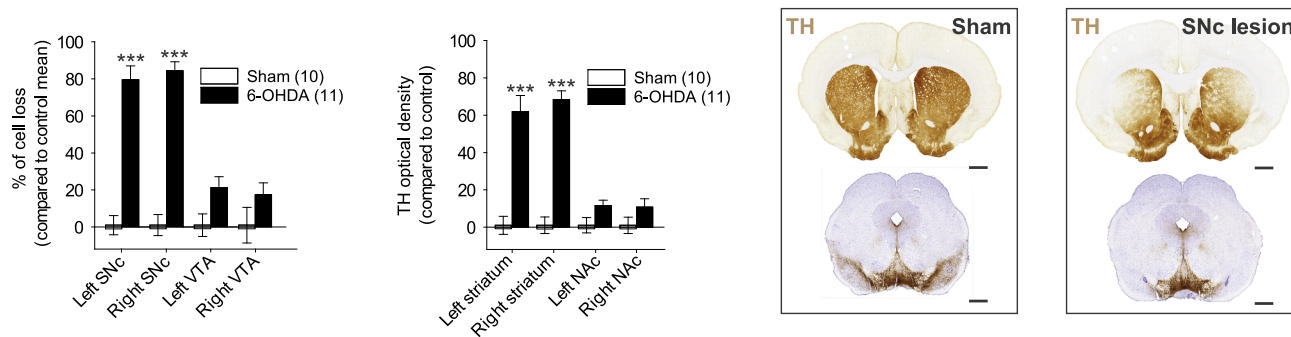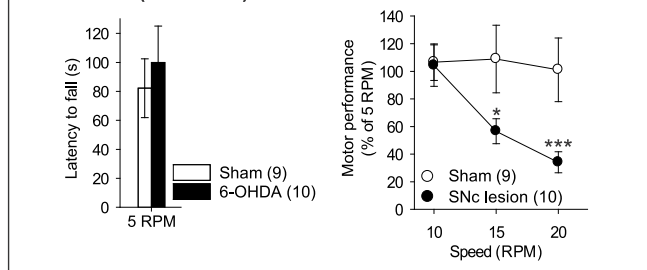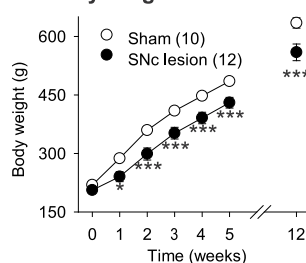
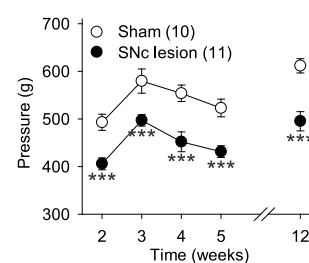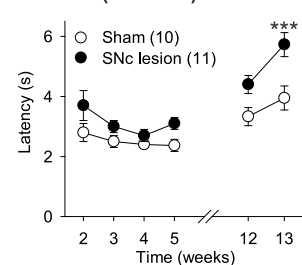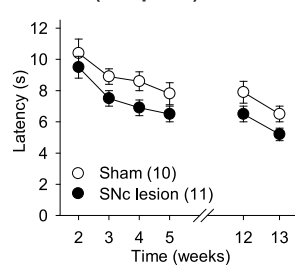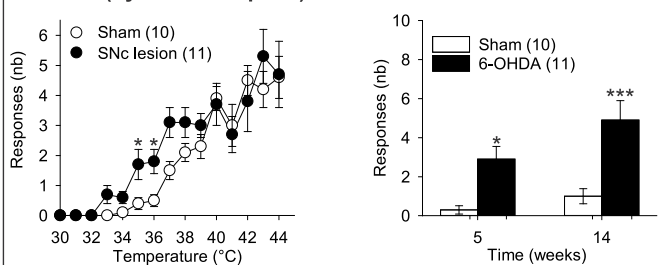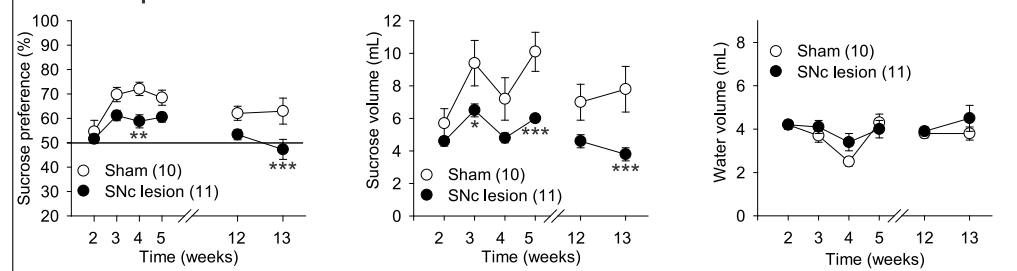**Fig. 2.** Effect of bilateral SNc lesion on motor and non-motor symptoms. Rats underwent SNc lesion (6-OHDA) and consequences were tested on motor (rotarod) and non-motor symptoms (body weight, digital forceps, tail flick, hot plate, dynamic hot plate and sucrose preference). (A) The bilateral partial lesion of the SNc led to a partial TH loss in the striatum. Scale bars, 1 mm. (B) SNc lesioned animals displayed motor deficits in the rotarod task (15 and 20 RPM). (C) The body weight of SNc lesioned animals remained lower than sham animals along the experiment. (D) SNc lesioned animals had a lower mechanical nociceptive threshold in a digital forceps test. (E) SNc lesioned animals showed a mild slowdown of the withdrawal response in the tail flick test, but a tendency at each test day for faster response in the classical hot plate test (F). (G) In the dynamic hot plate test, SNc lesioned animals respond to lower temperature than sham animals (left panel). Likewise, the comparison of the cumulative responses observed between 33 °C and 36 °C showed that lesioned animals exhibited higher number of nociceptive responses at normally non-nociceptive temperatures than control animals (right panel). (H) In a two-bottle-choice paradigm, lesioned animals showed a lower preference to sucrose solution (1%) compared to sham animals at 4 and 13 weeks after surgery (left panel). They also showed a decrease in sucrose consumption volume at 3, 5 and 13 weeks (middle panel) but not in water consumption (right panel). The number of animals is given between brackets. Values are presented as mean ± SEM (note that some SEMs are smaller than the symbol diameter, as for body weight for example). (*, $P < .05$; **, $P < .01$; ***; $P < .005$).

Regarding the motor symptoms, the bilateral lesion of the SNc induced the expected motor impairment in the rotarod task. Beside this motor influence, we also explored the impact of SNc lesion on some non-motor symptoms of Parkinson's disease (Faivre et al., 2019). The animals displayed lower mechanical nociceptive thresholds as assessed using digital forceps, which is similar to previous reports with other models and tests (Domenici et al., 2019; Gee et al., 2015; Zengin-Toktas et al., 2013), although some authors described that this effect may be time-dependent (Cao et al., 2016; Wang et al., 2017) or even side-dependent in case of unilateral lesion (Takeda et al., 2014). We also
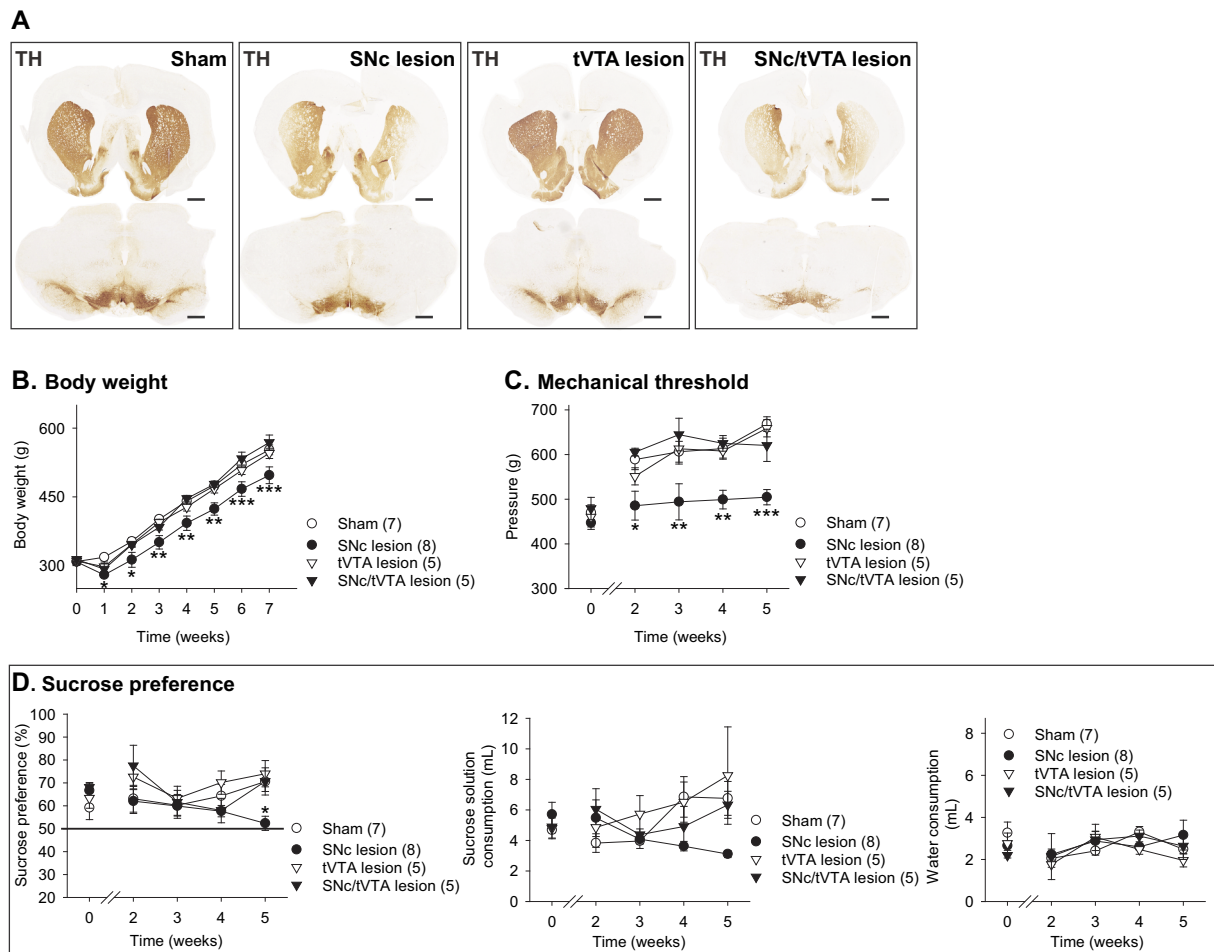
Fig. 3. Effect of bilateral tVTA lesion on non-motor symptoms in a model of Parkinson's disease. Animal underwent SNc lesion (6-OHDA) and/or tVTA excitotoxic lesion (ibotenic acid). The impact was studied on body weight, on nociceptive response to digital forceps and in the sucrose preference test. (A) The bilateral partial lesion of the SNc, but not of the tVTA alone, led to a partial TH loss in the striatum and the midbrain. Scale bars, 1 mm. (B) The body weight of SNc lesioned animals remained lower than other groups along the experiment. Animals with SNc and tVTA co-lesions showed similar body weight as control animals. (C) SNc lesioned animals showed lower mechanical nociceptive thresholds in the digital forceps test at all considered time points, which was compensated by concomitant lesion of the tVTA. (D) SNc lesioned animals showed a lower preference to sucrose compared to sham animals at 5 weeks after surgery (left panel), and a tendency to decreased overall sucrose (middle panel) but not water (right panel) consumption. As for other tests, the tVTA bilateral lesion compensated sucrose preference in SNc lesioned animals. The number of animals is given between brackets. Values are presented as mean ± SEM (note that some SEMs are smaller than the symbol diameter, as for body weight for example). (*, $P < .05$; **, $P < .01$; ***; $P < .005$).

assessed heat sensitivity but obtained some contradictory results, with an apparent hyposensitivity in the tail flick test, a tendency to hypersensitivity in the hot plate test and a thermal allodynia in the dynamic hot plate. Interestingly, such discrepancies also exist in the literature, particularly concerning the tail flick test for which results vary depending on the model, species and test procedure (Domenici et al., 2019; Faivre et al., 2019; Gee et al., 2015; Gómez-Paz et al., 2018; Greco et al., 2008; Grossmann et al., 1973; Nascimento et al., 2018; Ogata et al., 2015; Park et al., 2015; Tassorelli et al., 2007). Concerning the hot plate test, it has been documented that the response latency is decreased in 6-OHDA models of Parkinson's disease (Chen et al., 2013; Dolatshahi et al., 2015; Gee et al., 2015; Lin et al., 1981; Nascimento et al., 2018; Saadé et al., 1997). An explanation for these differences between tests may be related to the spinal reflex component of the tail flick, which is predominant in this test and influenced by descending supraspinal controls. The motor slow-down accompanying Parkinson's disease (Low et al., 2002; Mazzoni et al., 2012) and its models (Lindner et al., 1999; Santana et al., 2015) may thus mask in some protocols the nociceptive hypersensitivity. This technical limitation can however be overcome by using a slow ramp of temperature increment and by looking at the number of nociceptive responses instead of latencies.

This procedure thus allowed us detecting thermal allodynia (*i.e.* a pain-related response due to a stimulus that does not normally provoke pain) in the 6-OHDA lesioned animals. Finally, we assessed a symptom associated with depressive-like behaviors in animals, by using a sucrose preference test, and we observed a decreased preference with 6-OHDA lesion, in agreement with literature reports (Carvalho et al., 2013; Ilkiw et al., 2019; Kamińska et al., 2017; Liu et al., 2015; Matheus et al., 2016; Santiago et al., 2010, 2014; Silva et al., 2016; Tadaiesky et al., 2008; Vecchia et al., 2018). This effect was however time dependent (Matheus et al., 2016; Santiago et al., 2010), and displayed some variability from one experiment to the other, which required an appropriate time-window to detect it and thus makes it more challenging to systematically assess in the animal model. A motor impairment consecutive to 6-OHDA lesion could potentially also impair swallowing, which could then affect fluid intake (and thus sucrose consumption) and also lead to the body weight loss observed. However, at the considered time-points, the total amount of water consumed was equivalent between the experimental groups, supporting the fact that the observed decrease in sucrose preference was not a simple consequence of motor deficits.

Following co-lesion of the tVTA and the SNc, we observed that

animals exhibited the same motor performance, weight increase, nociceptive mechanical threshold and sucrose preference as control animals.

The bilateral lesion of the tVTA increased *per se* the motor performance of the animals at days 2 and 3 of rotarod testing, showing that the tVTA controls motor behaviors. This is in agreement with our previous report concerning the impact of tVTA lesion on motor performance and motor skill learning, which supports a main role of the tVTA as a GABA brake for the nigrostriatal pathway (Bourdy et al., 2014). The tVTA control over SNc dopamine neurons has been demonstrated by using neuroanatomical (Bourdy et al., 2014; Ferreira et al., 2008; Jhou et al., 2009a, 2009b; Kaufling et al., 2010a) and *in vivo* electrophysiological approaches (Bourdy et al., 2014), thus highlighting a tVTA-nigrostriatal pathway and the inhibitory influence of the tVTA on the activity of SNc dopamine neurons. Indeed, the electrical/chemical stimulation and chemical inhibition of the tVTA decreased and increased, respectively, the activity of the SNc dopamine neurons (Bourdy et al., 2014). Dopamine cells being under the control of excitatory and inhibitory inputs that regulate their activity (Gantz et al., 2018; Morikawa and Paladini, 2011), suppressing the inhibitory influence of the tVTA on dopamine cells may facilitate excitatory impact and promote activity of these cells. Accordingly, the bilateral lesion of the tVTA has been shown to increase the basal activity of the SNc dopamine neurons (Bourdy et al., 2014), even though no locomotor hyperactivity was present following such lesion (Bourdy et al., 2014; Jhou et al., 2009a). Such inhibitory control is also supported by previous findings showing that an unilateral lesion of the tVTA elicited an amphetamine-induced contralateral rotation bias, and compensated for the ipsilateral bias in animal with unilateral SNc lesion (Bourdy et al., 2014). In the present study, the concomitant bilateral lesion of the tVTA in animals with a bilateral partial SNc lesion improved motor performance, leading to similar level of motor performance as controls in the rotarod task. After SNc lesion, this action of tVTA lesion could be related to the loss of the inhibitory brake on the surviving dopamine neurons, and to the strong overlap of the terminal field of individual dopamine neurons within the striatal complex. Indeed, a single SNc neuron can, by its profuse arborisation (Gauthier et al., 1999; Matsuda et al., 2009; Prensa and Parent, 2001), cover up to 5.7% of the total volume of the striatum (Matsuda et al., 2009).

To assess tVTA influence on non-motor symptoms in the 6-OHDA model, we selected 3 parameters: the body weight, the mechanical nociceptive response assessed by the digital forceps test, and the sucrose preference test for the depressive-like behavior. The lesion of the tVTA had, *per se*, no impact on these parameters in animals with intact dopamine systems. It suggests that this brain region may not be essential to these functions and behaviors. It can however modulate them. Indeed, the tVTA lesion counterbalanced the weight loss, mechanical hypersensitivity and sucrose anhedonia in animals with bilateral SNc lesion, showing that tVTA can notably influence non-motor symptoms associated with partial loss of dopamine cells. The link between Parkinson's disease and weight loss in animal models has been associated with lower density of nigrostriatal dopamine neurons (Lee et al., 2016) and decreased striatal dopaminergic activity (Pak et al., 2018). Moreover, a low intensity deep brain stimulation of the tVTA significantly decreases rat's food intake (Melse et al., 2016). Unfortunately, we did not measure food intake itself throughout the experiments, which could have provided interesting information to relate to body weight changes. The influence of dopamine systems on nociceptive responses is also well established. Indeed, activation of mesolimbic neurons can mediate a suppression of tonic pain (Altier and Stewart, 1999; Wood, 2008), and the application of a dopamine D2 receptor agonist into the NAc has an antinociceptive action in the formalin test (Taylor et al., 2003). Moreover, the acute inhibition of the tVTA can have an analgesic action in the formalin test (Jhou et al., 2012), and the control of dopamine neurons by the tVTA is altered in a context of neuropathic pain (Sagheddu et al., 2015). Dopamine activity

is also altered in animal models of depression (Kaufling, 2019), and anatomical data and experimental evidence have also related the tVTA with depressive-like behaviors. Indeed, shocks provided according to a procedure usually leading to learned helplessness led to Fos induction in the tVTA (Brown and Shepard, 2013) and the lesion of this brain region decreased the number of escape failures (Brown and Shepard, 2013; Elmer et al., 2019). The loss of the tonic inhibitory control that the tVTA exerts on dopamine neurons (as well as on some serotonergic neurons) could contribute to the compensatory effect observed on these symptoms in the model of Parkinson's disease.

The present study provides behavioral evidence for a main influence of the tVTA on the expression of motor and non-motor symptoms related to partial loss of dopamine cells. While a co-lesional approach would be of poor therapeutic interest, the recent report of the molecular profile of the tVTA (Smith et al., 2019) may open other options. It might indeed help looking for potential pharmacological targets that could help modulating tVTA activity and thus positively influence symptoms in Parkinson's disease.

Author contributions

F·F and M.J.S.C. designed and performed experiments, analyzed data and drafted the manuscript; S.D. and S.B. performed experiments and analyzed data for quantification of 6-OHDA lesion; A.J. performed experiments; E.B. supervised 6-OHDA lesion analysis and drafted the manuscript; M.B. designed the study and drafted the manuscript.

Data accessibility

All data presented in the current manuscript can be obtained from the corresponding author.

Funding

Declaration of Competing Interest

None.

Acknowledgment

References

Alberico, S.L., Cassell, M.D., Narayanan, N.S., 2015. The vulnerable ventral tegmental area in Parkinson's disease. Basal Ganglia 5, 51–55. https://doi.org/10.1016/j.baga.2015.06.001.

Altier, N., Stewart, J., 1999. The role of dopamine in the nucleus accumbens in analgesia. Life Sci. 65, 2269–2287. https://doi.org/10.1016/S0024-3205(99)00298-2.

Antonini, A., Tinazzi, M., Abbruzzese, G., Berardelli, A., Chaudhuri, K.R., Defazio, G., Ferreira, J., Martinez-Martin, P., Trenkwalder, C., Rascol, O., 2018. Pain in Parkinson's disease: facts and uncertainties. Eur. J. Neurol. 25, 697–969. https://doi.org/10.1111/ene.13624.

Barrot, M., 2012. Tests and models of nociception and pain in rodents. Neuroscience 211, 39–50. https://doi.org/10.1016/j.neuroscience.2011.12.041.

Bezard, E., Przedborski, S., 2011. A tale on animal models of Parkinson's disease. Mov. Disord. 26, 993–1002. https://doi.org/10.1002/mds.23696.

Bezard, E., Yue, Z., Kirik, D., Spillantini, M.G., 2013. Animal models of Parkinson's disease: limits and relevance to neuroprotection studies. Mov. Disord. 28, 61–70.

https://doi.org/10.1002/mds.25108.

Blanchet, P.J., Brefel-Courbon, C., 2017. Chronic pain and pain processing in Parkinson's disease. Prog. Neuro-Psychopharmacol. Biol. Psychiatry. https://doi.org/10.1016/j.pnpbp.2017.10.010.

Bonito-Oliva, A., Masini, D., Fisone, G., 2014. A mouse model of non-motor symptoms in Parkinson's disease: focus on pharmacological interventions targeting affective dysfunctions. Front. Behav. Neurosci. 8, 290. https://doi.org/10.3389/fnbeh.2014.00290.

Bourdenx, M., Dovero, S., Engeln, M., Bido, S., Bastide, M.F., Dutheil, N., Vollenweider, I., Baud, L., Piron, C., Grouthier, V., Boraud, T., Porras, G., Li, Q., Baekelandt, V., Scheller, D., Michel, A., Fernagut, P.-O., Georges, F., Courtine, G., Bezard, E., Dehay, B., 2015. Lack of additive role of ageing in nigrostriatal neurodegeneration triggered by α-synuclein overexpression. Acta Neuropathol. Commun. 3, 46. https://doi.org/10.1186/s40478-015-0222-2.

Bourdy, R., Barrot, M., 2012. A new control center for dopaminergic systems: pulling the VTA by the tail. Trends Neurosci. 35, 681–690. https://doi.org/10.1016/j.tins.2012.06.007.

Bourdy, R., Sánchez-Catalán, M.-J., Kaufling, J., Balcita-Pedicino, J.J., Freund-Mercier, M.-J., Veinante, P., Sesack, S.R., Georges, F., Barrot, M., 2014. Control of the nigrostriatal dopamine neuron activity and motor function by the tail of the ventral tegmental area. Neuropsychopharmacology 39, 2788–2798. https://doi.org/10.1038/npp.2014.129.

Bové, J., Prou, D., Perier, C., Przedborski, S., 2005. Toxin-induced models of Parkinson's disease. NeuroRx 2, 484–494. https://doi.org/10.1602/neurorx.2.3.484.

Brown, P.L., Shepard, P.D., 2013. Lesions of the fasciculus retroflexus alter footshock-induced cFos expression in the mesopontine rostromedial tegmental area of rats. PLoS One 8, e60678. https://doi.org/10.1371/journal.pone.0060678.

Cao, L.-F., Peng, X.-Y., Huang, Y., Wang, B., Zhou, F.-M., Cheng, R.-X., Chen, L.-H., Luo, W.-F., Liu, T., 2016. Restoring spinal noradrenergic inhibitory tone attenuates pain hypersensitivity in a rat model of Parkinson's disease. Neural Plast. 2016, 6383240. https://doi.org/10.1155/2016/6383240.

Carvalho, M.M., Campos, F.L., Coimbra, B., Pêgo, J.M., Rodrigues, C., Lima, R., Rodrigues, A.J., Sousa, N., Salgado, A.J., 2013. Behavioral characterization of the 6-hydroxidopamine model of Parkinson's disease and pharmacological rescuing of non-motor deficits. Mol. Neurodegener. 8, 14. https://doi.org/10.1186/1750-1326-8-14.

Chaudhuri, K.R., Healy, D.G., Schapira, A.H.V., National Institute for Clinical Excellence, 2006. Non-motor symptoms of Parkinson's disease: diagnosis and management. Lancet Neurol. 5, 235–245. https://doi.org/10.1016/S1474-4422(06)70373-8.

Chen, C.-C.V., Shih, Y.-Y.I., Chang, C., 2013. Dopaminergic imaging of nonmotor manifestations in a rat model of Parkinson's disease by fMRI. Neurobiol. Dis. 49, 99–106. https://doi.org/10.1016/j.nbd.2012.07.020.

da Silva, T.P., Poli, A., Hara, D.B., Takahashi, R.N., 2016. Time course study of microglial and behavioral alterations induced by 6-hydroxydopamine in rats. Neurosci. Lett. 622, 83–87. https://doi.org/10.1016/j.neulet.2016.04.049.

Dauer, W., Przedborski, S., 2003. Parkinson's disease: mechanisms and models. Neuron 39, 889–909. https://doi.org/10.1016/s0896-6273(03)00568-3.

Dolatshahi, M., Farbood, Y., Sarkaki, A., Mansouri, S.M.T., Khodadadi, A., 2015. Ellagic acid improves hyperalgesia and cognitive deficiency in 6-hydroxidopamine induced rat model of Parkinson's disease. Iran. J. Basic Med. Sci. 18, 38–46.

Domenici, R.A., Campos, A.C.P., Maciel, S.T., Berzuino, M.B., Hernandes, M.S., Fonoff, E.T., Pagano, R.L., 2019. Parkinson's disease and pain: modulation of nociceptive circuitry in a rat model of nigrostriatal lesion. Exp. Neurol. 315, 72–81. https://doi.org/10.1016/j.expneurol.2019.02.007.

Elmer, G.I., Palacorolla, H., Mayo, C.L., Brown, P.L., Jhou, T.C., Brady, D., Shepard, P.D., 2019. The rostromedial tegmental nucleus modulates the development of stress-induced helpless behavior. Behav. Brain Res. 359, 950–957. https://doi.org/10.1016/j.bbr.2018.06.014.

Faivre, F., Joshi, A., Bezard, E., Barrot, M., 2019. The hidden side of Parkinson's disease: studying pain, anxiety and depression in animal models. Neurosci. Biobehav. Rev. 96, 335–352. https://doi.org/10.1016/j.neubiorev.2018.10.004.

Ferreira, J.G.P., Del-Fava, F., Hasue, R.H., Shammah-Lagnado, S.J., 2008. Organization of ventral tegmental area projections to the ventral tegmental area-nigral complex in the rat. Neuroscience 153, 196–213. https://doi.org/10.1016/j.neuroscience.2008.02.003.

Gantz, S.C., Ford, C.P., Morikawa, H., Williams, J.T., 2018. The evolving understanding of dopamine neurons in the Substantia Nigra and ventral tegmental area. Annu. Rev. Physiol. 80, 219–241. https://doi.org/10.1146/annurev-physiol-021317-121615.

Gauthier, J., Parent, M., Lévesque, M., Parent, A., 1999. The axonal arborization of single nigrostriatal neurons in rats. Brain Res. 834, 228–232. https://doi.org/10.1016/s0006-8993(99)01573-5.

Gee, L.E., Chen, N., Ramirez-Zamora, A., Shin, D.S., Pilitsis, J.G., 2015. The effects of subthalamic deep brain stimulation on mechanical and thermal thresholds in 6OHDA-lesioned rats. Eur. J. Neurosci. 42, 2061–2069. https://doi.org/10.1111/ejn.12992.

German, D.C., Manaye, K., Smith, W.K., Woodward, D.J., Saper, C.B., 1989. Midbrain dopaminergic cell loss in Parkinson's disease: computer visualization. Ann. Neurol. 26, 507–514. https://doi.org/10.1002/ana.410260403.

Gómez-Paz, A., Drucker-Colín, R., Milán-Aldaco, D., Palomero-Rivero, M., Ambriz-Tututi, M., 2018. Intrastriatal chromospheres' transplant reduces nociception in hemiparkinsonian rats. Neuroscience 387, 123–134. https://doi.org/10.1016/j.neuroscience.2017.08.052.

Greco, R., Tassorelli, C., Armentero, M.T., Sandrini, G., Nappi, G., Blandini, F., 2008. Role of central dopaminergic circuitry in pain processing and nitroglycerin-induced hyperalgesia. Brain Res. 1238, 215–223. https://doi.org/10.1016/j.brainres.2008.08.022.

Grossmann, W., Jurna, I., Nell, T., Theres, C., 1973. The dependence of the anti-

nociceptive effect of morphine and other analgesic agents on spinal motor activity after central monoamine depletion. Eur. J. Pharmacol. 24, 67–77. https://doi.org/10.1016/0014-2999(73)90115-5.

Gubellini, P., Kachidian, P., 2015. Animal models of Parkinson's disease: an updated overview. Rev. Neurol. (Paris) 171, 750–761. https://doi.org/10.1016/j.neurol.2015.07.011.

Hong, S., Jhou, T.C., Smith, M., Saleem, K.S., Hikosaka, O., 2011. Negative reward signals from the lateral habenula to dopamine neurons are mediated by rostromedial tegmental nucleus in primates. J. Neurosci. 31, 11457–11471. https://doi.org/10.1523/JNEUROSCI.1384-11.2011.

Ilkiw, J.L., Kmita, L.C., Targa, A.D.S., Noseda, A.C.D., Rodrigues, L.S., Dorieux, F.W.C., Fagotti, J., Dos Santos, P., Lima, M.M.S., 2019. Dopaminergic lesion in the olfactory bulb restores olfaction and induces depressive-like Behaviors in a 6-OHDA model of Parkinson's disease. Mol. Neurobiol. 56, 1082–1095. https://doi.org/10.1007/s12035-018-1134-5.

Jalabert, M., Bourdy, R., Courtin, J., Veinante, P., Manzoni, O.J., Barrot, M., Georges, F., 2011. Neuronal circuits underlying acute morphine action on dopamine neurons. Proc. Natl. Acad. Sci. U. S. A. 108, 16446–16450. https://doi.org/10.1073/pnas.1105418108.

Jhou, T.C., Fields, H.L., Baxter, M.G., Saper, C.B., Holland, P.C., 2009a. The rostromedial tegmental nucleus (RMTg), a GABAergic afferent to midbrain dopamine neurons, encodes aversive stimuli and inhibits motor responses. Neuron 61, 786–800. https://doi.org/10.1016/j.neuron.2009.02.001.

Jhou, T.C., Geisler, S., Marinelli, M., Degarmo, B.A., Zahm, D.S., 2009b. The mesopontine rostromedial tegmental nucleus: a structure targeted by the lateral habenula that projects to the ventral tegmental area of Tsai and substantia nigra compacta. J. Comp. Neurol. 513, 566–596. https://doi.org/10.1002/cne.21891.

Jhou, T.C., Xu, S.-P., Lee, M.R., Gallen, C.L., Ikemoto, S., 2012. Mapping of reinforcing and analgesic effects of the mu opioid agonist endomorphin-1 in the ventral midbrain of the rat. Psychopharmacology 224, 303–312. https://doi.org/10.1007/s00213-012-2753-6.

Jhou, T.C., Good, C.H., Rowley, C.S., Xu, S.-P., Wang, H., Burnham, N.W., Hoffman, A.F., Lupica, C.R., Ikemoto, S., 2013. Cocaine drives aversive conditioning via delayed activation of dopamine-responsive habenular and midbrain pathways. J. Neurosci. 33, 7501–7512. https://doi.org/10.1523/JNEUROSCI.3634-12.2013.

Kamińska, K., Lenda, T., Konieczny, J., Czarnecka, A., Lorenc-Koci, E., 2017. Depressive-like neurochemical and behavioral markers of Parkinson's disease after 6-OHDA administered unilaterally to the rat medial forebrain bundle. Pharmacol. Rep. PR 69, 985–994. https://doi.org/10.1016/j.pharep.2017.05.016.

Kaufling, J, 2019. Alterations and adaptation of ventral tegmental area dopaminergic neurons in animal models of depression. Cell Tissue Res. 377, 59–71. https://doi.org/10.1007/s00441-019-03007-9.

Kaufling, J., Aston-Jones, G., 2015. Persistent adaptations in afferents to ventral tegmental dopamine neurons after opiate withdrawal. J. Neurosci. 35, 10290–10303. https://doi.org/10.1523/JNEUROSCI.0715-15.2015.

Kaufling, J., Veinante, P., Pawlowski, S.A., Freund-Mercier, M.-J., Barrot, M., 2009. Afferents to the GABAergic tail of the ventral tegmental area in the rat. J. Comp. Neurol. 513, 597–621. https://doi.org/10.1002/cne.21983.

Kaufling, J., Veinante, P., Pawlowski, S.A., Freund-Mercier, M.-J., Barrot, M., 2010a. gamma-Aminobutyric acid cells with cocaine-induced DeltaFosB in the ventral tegmental area innervate mesolimbic neurons. Biol. Psychiatry 67, 88–92. https://doi.org/10.1016/j.biopsych.2009.08.001.

Kaufling, J., Waltisperger, E., Bourdy, R., Valera, A., Veinante, P., Freund-Mercier, M.-J., Barrot, M., 2010b. Pharmacological recruitment of the GABAergic tail of the ventral tegmental area by acute drug exposure. Br. J. Pharmacol. 161, 1677–1691. https://doi.org/10.1111/j.1476-5381.2010.00984.x.

Lecca, S., Melis, M., Luchicchi, A., Ennas, M.G., Castelli, M.P., Muntoni, A.L., Pistis, M., 2011. Effects of drugs of abuse on putative rostromedial tegmental neurons, inhibitory afferents to midbrain dopamine cells. Neuropsychopharmacology 36, 589–602. https://doi.org/10.1038/npp.2010.190.

Lecca, S., Melis, M., Luchicchi, A., Muntoni, A.L., Pistis, M., 2012. Inhibitory inputs from rostromedial tegmental neurons regulate spontaneous activity of midbrain dopamine cells and their responses to drugs of abuse. Neuropsychopharmacology 37, 1164–1176. https://doi.org/10.1038/npp.2011.302.

Lee, J.J., Oh, J.S., Ham, J.H., Lee, D.H., Lee, I., Sohn, Y.H., Kim, J.S., Lee, P.H., 2016. Association of body mass index and the depletion of nigrostriatal dopamine in Parkinson's disease. Neurobiol. Aging 38, 197–204. https://doi.org/10.1016/j.neurobiolaging.2015.11.009.

Li, H., Pullmann, D., Cho, J.Y., Eid, M., Jhou, T.C., 2019. Generality and opponency of rostromedial tegmental (RMTg) roles in valence processing. eLife 8. https://doi.org/10.7554/eLife.41542.

Lin, M.T., Wu, J.J., Chandra, A., Tsay, B.L., 1981. Activation of striatal dopamine receptors induces pain inhibition in rats. J. Neural Transm. 51, 213–222.

Lindner, M.D., Cain, C.K., Plone, M.A., Frydel, B.R., Blaney, T.J., Emerich, D.F., Hoane, M.R., 1999. Incomplete nigrostriatal dopaminergic cell loss and partial reductions in striatal dopamine produce akinesia, rigidity, tremor and cognitive deficits in middle-aged rats. Behav. Brain Res. 102, 1–16. https://doi.org/10.1016/s0166-4328(98)00160-0.

Liu, K.-C., Li, J.-Y., Tan, H.-H., Du, C.-X., Xie, W., Zhang, Y.-M., Ma, W.-L., Zhang, L., 2015. Serotonin₆ receptors in the dorsal hippocampus regulate depressive-like behaviors in unilateral 6-hydroxydopamine-lesioned Parkinson's rats. Neuropharmacology 95, 290–298. https://doi.org/10.1016/j.neuropharm.2015.03.031.

Low, K.A., Miller, J., Vierck, E., 2002. Response slowing in Parkinson's disease: a psychophysiological analysis of premotor and motor processes. Brain J. Neurol. 125, 1980–1994. https://doi.org/10.1093/brain/awf206.

Luis-Delgado, O.E., Barrot, M., Rodeau, J.-L., Schott, G., Benbouzid, M., Poisbeau, P., Freund-Mercier, M.-J., Lasbennes, F., 2006. Calibrated forceps: a sensitive and reliable tool for pain and analgesia studies. J. Pain 7, 32–39. https://doi.org/10.1016/j.jpain.2005.07.011.

Marsili, L., Rizzo, G., Colosimo, C., 2018. Diagnostic criteria for Parkinson's disease: from James Parkinson to the concept of prodromal disease. Front. Neurol. 9, 156. https://doi.org/10.3389/fneur.2018.00156.

Matheus, F.C., Rial, D., Real, J.I., Lemos, C., Takahashi, R.N., Bertoglio, L.J., Cunha, R.A., Prediger, R.D., 2016. Temporal dissociation of striatum and prefrontal cortex uncouples Anhedonia and Defense Behaviors relevant to depression in 6-OHDA-Lesioned rats. Mol. Neurobiol. 53, 3891–3899. https://doi.org/10.1007/s12035-015-9330-z.

Matsuda, W., Furuta, T., Nakamura, K.C., Hioki, H., Fujiyama, F., Arai, R., Kaneko, T., 2009. Single nigrostriatal dopaminergic neurons form widely spread and highly dense axonal arborizations in the neostriatum. J. Neurosci. 29, 444–453. https://doi.org/10.1523/JNEUROSCI.4029-08.2009.

Matsui, A., Williams, J.T., 2011. Opioid-sensitive GABA inputs from rostromedial tegmental nucleus synapse onto midbrain dopamine neurons. J. Neurosci. 31, 17729–17735. https://doi.org/10.1523/JNEUROSCI.4570-11.2011.

Mazzoni, P., Shabbott, B., Cortés, J.C., 2012. Motor control abnormalities in Parkinson's disease. Cold Spring Harb. Perspect. Med. 2, a009282. https://doi.org/10.1101/cshperspect.a009282.

Melse, M., Temel, Y., Tan, S.K., Jahanshahi, A., 2016. Deep brain stimulation of the rostromedial tegmental nucleus: an unanticipated, selective effect on food intake. Brain Res. Bull. 127, 23–28. https://doi.org/10.1016/j.brainresbull.2016.08.004.

Morikawa, H., Paladini, C.A., 2011. Dynamic regulation of midbrain dopamine neuron activity: intrinsic, synaptic, and plasticity mechanisms. Neuroscience 198, 95–111. https://doi.org/10.1016/j.neuroscience.2011.08.023.

Nascimento, G.C., Bariotto-Dos-Santos, K., Leite-Panissi, C.R.A., Del-Bel, E.A., Bortolanza, M., 2018. Nociceptive response to L-DOPA-induced dyskinesia in Hemiparkinsonian rats. Neurotox. Res. 34, 799–807. https://doi.org/10.1007/s12640-018-9896-0.

Ogata, M., Noda, K., Akita, H., Ishibashi, H., 2015. Characterization of nociceptive response to chemical, mechanical, and thermal stimuli in adolescent rats with neonatal dopamine depletion. Neuroscience 289, 43–55. https://doi.org/10.1016/j.neuroscience.2015.01.002.

Pak, K., Shin, H.K., Kim, E.-J., Lee, J.-H., Lyoo, C.H., Son, J., Lee, M.J., 2018. Weight loss is associated with rapid striatal dopaminergic degeneration in Parkinson's disease. Parkinsonism Relat. Disord. 51, 67–72. https://doi.org/10.1016/j.parkreldis.2018.02.044.

Park, A., Stacy, M., 2009. Non-motor symptoms in Parkinson's disease. J. Neurol. 256 (Suppl. 3), 293–298. https://doi.org/10.1007/s00415-009-5240-1.

Park, J., Lim, C.-S., Seo, H., Park, C.-A., Zhuo, M., Kaang, B.-K., Lee, K., 2015. Pain perception in acute model mice of Parkinson's disease induced by 1-methyl-4-phenyl-1,2,3,6-tetrahydropyridine (MPTP). Mol. Pain 11, 28. https://doi.org/10.1186/s12990-015-0026-1.

Paxinos, G., Watson, C., 2014. The Rat Brain in Stereotaxic Coordinates. Academic Press.

Perrotti, L.I., Bolaños, C.A., Choi, K.-H., Russo, S.J., Edwards, S., Ulery, P.G., Wallace, D.L., Self, D.W., Nestler, E.J., Barrot, M., 2005. DeltaFosB accumulates in a GABAergic cell population in the posterior tail of the ventral tegmental area after psychostimulant treatment. Eur. J. Neurosci. 21, 2817–2824. https://doi.org/10.1111/j.1460-9568.2005.04110.x.

Prensa, L., Parent, A., 2001. The nigrostriatal pathway in the rat: a single-axon study of the relationship between dorsal and ventral tier nigral neurons and the striosome/matrix striatal compartments. J. Neurosci. 21, 7247–7260. https://doi.org/10.1523/JNEUROSCI.21-18-07247.2001.

Saadé, N.E., Atweh, S.F., Bahuth, N.B., Jabbur, S.J., 1997. Augmentation of nociceptive reflexes and chronic deafferentation pain by chemical lesions of either dopaminergic terminals or midbrain dopaminergic neurons. Brain Res. 751, 1–12. https://doi.org/10.1016/s0006-8993(96)01164-x.

Sagheddu, C., Aroni, S., De Felice, M., Lecca, S., Luchicchi, A., Melis, M., Muntoni, A.L., Romano, R., Palazzo, E., Guida, F., Maione, S., Pistis, M., 2015. Enhanced serotonin and mesolimbic dopamine transmissions in a rat model of neuropathic pain. Neuropharmacology 97, 383–393. https://doi.org/10.1016/j.neuropharm.2015.06.003.

Sakai, K., Gash, D.M., 1994. Effect of bilateral 6-OHDA lesions of the substantia nigra on locomotor activity in the rat. Brain Res. 633, 144–150. https://doi.org/10.1016/0006-8993(94)91533-4.

Sanchez-Catalan, M.J., Kaufling, J., Georges, F., Veinante, P., Barrot, M., 2014. The antero-posterior heterogeneity of the ventral tegmental area. Neuroscience 282, 198–216. https://doi.org/10.1016/j.neuroscience.2014.09.025.

Sánchez-Catalán, M.-J., Faivre, F., Yalcin, I., Muller, M.-A., Massotte, D., Majchrzak, M., Barrot, M., 2017. Response of the tail of the ventral tegmental area to aversive stimuli. Neuropsychopharmacology 42, 638–648. https://doi.org/10.1038/npp.2016.139.

Santana, M., Palmér, T., Simplício, H., Fuentes, R., Petersson, P., 2015. Characterization of long-term motor deficits in the 6-OHDA model of Parkinson's disease in the common marmoset. Behav. Brain Res. 290, 90–101. https://doi.org/10.1016/j.bbr.2015.04.037.

Santiago, R.M., Barbieiro, J., Lima, M.M.S., Dombrowski, P.A., Andreatini, R., Vital, M.A.B.F., 2010. Depressive-like behaviors alterations induced by intranigral MPTP, 6-OHDA, LPS and rotenone models of Parkinson's disease are predominantly associated with serotonin and dopamine. Prog. Neuropsychopharmacol. Biol. Psychiatry 34, 1104–1114. https://doi.org/10.1016/j.pnpbp.2010.06.004.

Santiago, R.M., Barbiero, J., Gradowski, R.W., Bochen, S., Lima, M.M.S., Da Cunha, C., Andreatini, R., Vital, M.A.B.F., 2014. Induction of depressive-like behavior by intranigral 6-OHDA is directly correlated with deficits in striatal dopamine and hippocampal serotonin. Behav. Brain Res. 259, 70–77. https://doi.org/10.1016/j.bbr.2013.10.035.

Smith, R.J., Vento, P.J., Chao, Y.S., Good, C.H., Jhou, T.C., 2019. Gene expression and neurochemical characterization of the rostromedial tegmental nucleus (RMTg) in rats and mice. Brain Struct. Funct. 224, 219–238. https://doi.org/10.1007/s00429-018-1761-7.

Stamatakis, A.M., Stuber, G.D., 2012. Activation of lateral habenula inputs to the ventral midbrain promotes behavioral avoidance. Nat. Neurosci. 15, 1105–1107. https://doi.org/10.1038/nn.3145.

Tadaiesky, M.T., Dombrowski, P.A., Figueiredo, C.P., Cargnin-Ferreira, E., Da Cunha, C., Takahashi, R.N., 2008. Emotional, cognitive and neurochemical alterations in a premotor stage model of Parkinson's disease. Neuroscience 156, 830–840. https://doi.org/10.1016/j.neuroscience.2008.08.035.

Takeda, R., Ishida, Y., Ebihara, K., Abe, H., Matsuo, H., Ikeda, T., Koganemaru, G., Kuramashi, A., Funahashi, H., Magata, Y., Kawai, K., Nishimori, T., 2014. Intrastriatal grafts of fetal ventral mesencephalon improve allodynia-like withdrawal response to mechanical stimulation in a rat model of Parkinson's disease. Neurosci. Lett. 573, 19–23. https://doi.org/10.1016/j.neulet.2014.05.007.

Tassorelli, C., Armentero, M.-T., Greco, R., Fancellu, R., Sandrini, G., Nappi, G., Blandini, F., 2007. Behavioral responses and Fos activation following painful stimuli in a rodent model of Parkinson's disease. Brain Res. 1176, 53–61 doi:10.1016./j.brainres.2007.08.012.

Taylor, B.K., Joshi, C., Uppal, H., 2003. Stimulation of dopamine D2 receptors in the nucleus accumbens inhibits inflammatory pain. Brain Res. 987, 135–143. https://doi.org/10.1016/s0006-8993(03)03318-3.

Ungerstedt, U., 1968. 6-Hydroxy-dopamine induced degeneration of central monoamine neurons. Eur. J. Pharmacol. 5, 107–110.

Vecchia, D.D., Kanazawa, L.K.S., Wendler, E., de Almeida Soares Hocayen, P., Bruginski, E., Campos, F.R., Stern, C.A.J., Vital, M.A.B.F., Miyoshi, E., Wöhr, M., Schwarting, R.K.W., Andreatini, R., 2018. Effects of ketamine on vocal impairment, gait changes, and anhedonia induced by bilateral 6-OHDA infusion into the substantia nigra pars compacta in rats: therapeutic implications for Parkinson's disease. Behav. Brain Res. 342, 1–10. https://doi.org/10.1016/j.bbr.2017.12.041.

Vingill, S., Connor-Robson, N., Wade-Martins, R., 2018. Are rodent models of Parkinson's disease behaving as they should? Behav. Brain Res. 352, 133–141. https://doi.org/10.1016/j.bbr.2017.10.021.

Wang, C.-T., Mao, C.-J., Zhang, X.-Q., Zhang, C.-Y., Lv, D.-J., Yang, Y.-P., Xia, K.-L., Liu, J.-Y., Wang, F., Hu, L.-F., Xu, G.-Y., Liu, C.-F., 2017. Attenuation of hyperalgesia responses via the modulation of 5-hydroxytryptamine signalings in the rostral ventromedial medulla and spinal cord in a 6-hydroxydopamine-induced rat model of Parkinson's disease. Mol. Pain 13 https://doi.org/10.1177/1744806917691525. 1744806917691525.

Wood, P.B., 2008. Role of central dopamine in pain and analgesia. Expert. Rev. Neurother. 8, 781–797. https://doi.org/10.1586/14737175.8.5.781.

Yalcin, I., Charlet, A., Freund-Mercier, M.-J., Barrot, M., Poisbeau, P., 2009. Differentiating thermal Allodynia and Hyperalgesia using dynamic hot and cold plate in rodents. J. Pain 10, 767–773. https://doi.org/10.1016/j.jpain.2009.01.325.

Zengin-Toktas, Y., Ferrier, J., Durif, F., Llorca, P.-M., Authier, N., 2013. Bilateral lesions of the nigrostriatal pathways are associated with chronic mechanical pain hypersensitivity in rats. Neurosci. Res. 76, 261–264. https://doi.org/10.1016/j.neures.2013.05.003.